euronoise

A route to chaotic state on an electrodynamic loudspeaker

Antonio Petosic[a], Ivan Djurek[a] and Djurek Danijel[b]

[a]Faculty of Electrical Engineering and Computing, Unska 3, 10000 Zagreb, Croatia
[b]AVAC, Kesten brijeg 15, 10000 Zagreb, Croatia
antonio.petosic@fer.hr

The low frequency electrodynamic loudspeaker (EDL) unit has been analyzed in terms of chaotic behavior. It was found that an electrodynamic loudspeaker can function as a chaotic system. Loudspeaker impedance and vibration amplitude as function of driving frequency were measured at various excitation currents, and well-know cut-off effect from nonlinear dynamical systems has been observed. In the frequency region near cut-off frequency and at higher driving currents the period doubling and later chaotic state occur. The experimentally obtained chaotic state was confirmed theoretically solving 1-D nonlinear equation of motion with strong effective stiffness spatial dependency. It was found that statically measured suspension effective stiffness does not enable chaotic state when it is included in differential equation of motion. It has been concluded that membrane viscoelastic properties enhance the restoring force far enough to obtain chaos. The nonlinear equation describing anharmonic periodically driven oscillator with strong nonlinear effective stiffness has been solved numerically and some parameters showing chaotic state have been observed.

1 Introduction

Loudspeaker performance and their accuracy in reproducing an audio signal without adding distortion are significantly lower than that of other audio equipment. For example, harmonic distortion in a typical loudspeaker can be 100 to 1000 times greater than that of amplifiers. In a dynamic loudspeaker, sound is typically reproduced by the movement of a current-carrying object in a magnetic field due to the Lorentz force. The vibration of membrane causes the vibrations of air molecules in front of the loudspeaker and sound wave is generated.

A simplified model of an electrodynamic loudspeaker operates as a driven, damped harmonic oscillator. The dynamics of the displacement of the membrane x is given by the second order time-dependent ordinary differential equation (ODE) in the form of eq. 1 [1].

$$M_{eff} \cdot \frac{d^2x}{dt^2} + R_m \cdot \frac{dx}{dt} + k_{eff} \cdot x = B \cdot l \cdot I_0 \cdot \cos(\omega \cdot t) \quad (1)$$

M_{eff} [kg] - EDL effective mass (membrane + suspension mass)

R_m [kg/s] - mechanical losses in the system; internal suspension friction, membrane friction and friction coming from vibrating air

k_{eff} [N/m^2] - effective stiffness of loudspeaker suspension and membrane

B [T] - magnetic field

l [m] - length of voice coil wire in magnetic field

I_0 [A] - magnitude of excitation current

$\omega = 2 \cdot \pi \cdot f$ [s^{-1}] - radial frequency of excitation current

The frequency dependence of loudspeaker displacement and input electrical impedance near series resonance frequency has been measured using measurement system shown on fig. 1.

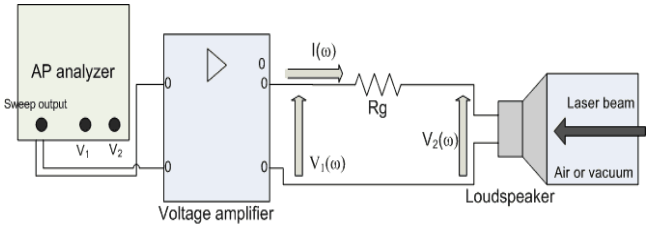

Fig.1 Measurement setup

The very good agreement between theoretical modeling and experimental results has been obtained at lower current magnitudes (up to 50 mA) [2,3]. The equivalent antireciprocal transducer circuit approach (fig. 2) has been compared with 1-D linear equation modeling (eq. 1). It has been concluded that parameters of model should be changed at each current excitation level I_0 to obtain good agreement between theoretical and experimental results.

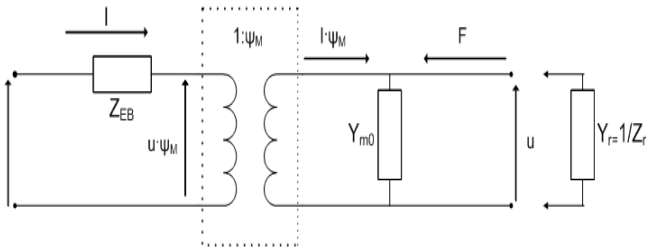

Fig. 2 Electrodynamic loudspeaker modeling as antireciprocal transducer

Comparison between experimental results and theoretical linear modeling using different approaches are shown on figure 3.

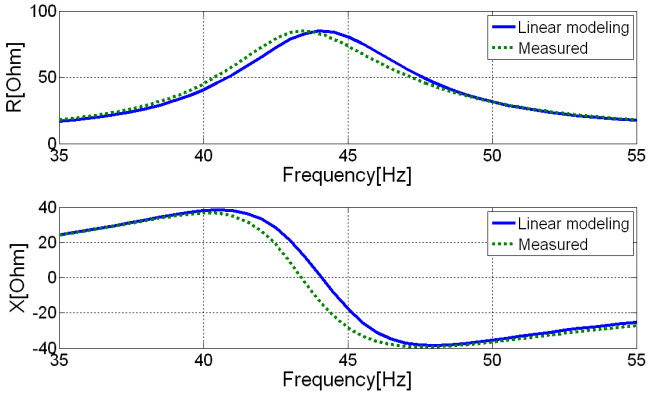

Fig. 3 Comparison between theoretical 1-D modeling and experimental results for real and imaginary part of electrical impedance at I_0= 50 mA

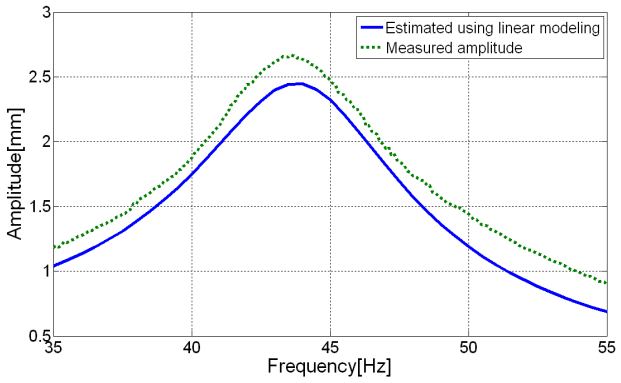

Fig. 4 Displacement amplitude (I_0=50 mA)

One of the effects observed is a decrease of resonant frequency with increasing excitation current as shown in figure 5. Linear model cannot give reasonable explanation for this effect.

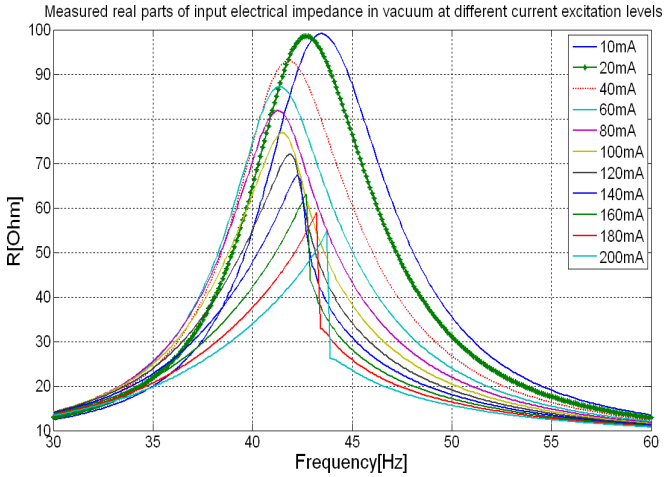

Fig. 5. Real part of electrical impedance frequency dependency vs. excitation current magnitude

It has been concluded that nonlinear dynamics have to been included in modeling of and EDL unit. Effective mass, stiffness and intrinsic friction spatial dependecy is suggested to use in nonlinear equation. Factor $B \cdot l$ does not have strong monlinear spatial dependency and it can be neglected up to 5mm displacement amplitudes.

2 Nonlinear EDL behaviour

First suggested model was in the form with effective mass, stiffness and intrinsic friction displacement dependency in the form of eq. 2

$$(M_{eff}(x)+\frac{X_s(\omega,x)}{\omega})\cdot\frac{d^2x}{dt^2}+(R_m(x)+Rs(\omega,x))\cdot\frac{dx}{dt}+k_{eff}(x)\cdot x = B\cdot l\cdot I_0\cdot\cos(\omega\cdot t)$$

Effective mass spatial dependency has form of S-function same as friction term R_m.

The real (R_s) and imaginary (X_S) part of radiation impedance should also be included in equation of motion when EDL is operating in air. The nonlinearity in these terms is due to effective radiation surface displacement dependency.

Simplified situation for experimental observation is when this terms are zero and EDL unit is operating in vacuum. In that case the real and imaginary part of radiation impedance can be neglected.

At lower excitation amplitudes only part of loudspeaker membrane is included in motion. At higher displacement amplitude the whole part of membrane is included in equation of motion. The cut-off effect and resonance frequency magnitude dependency can be theoretically modeled with this 1-D second order nonlinear equation of motion with appropriately included all nonlinearities.

In these experiments stiffness was evaluated in static measurements by the use of calibrated loads and corresponding evaluation of membrane displacements. It was found that effective stiffness is in the form $k_{eff}=m+n\cdot x+p\cdot x^2$, where coefficients m, n and p have these values: m=480 N/m, n=$-31\cdot10^3$ N/m^2, p=$7.5\cdot10^6$ N/m^3, and it is notable that k obeys a minimum value at x~2.07 mm.

A little consideration of Eq. 2 showed that it would be exceedingly difficult to explain amplitude bifurcations and chaotic state in EDL by this nonlinearity, even if coefficients m, n and p are varied in a broad range of values being far apart from the commonly accepted values indicated by technical performance of the loudspeaker. Instead, the only effect evaluated by the use of simulations based upon cubic nonlinearity was well known amplitude cut-off, continuously observed during the course of this work (Figure 6).

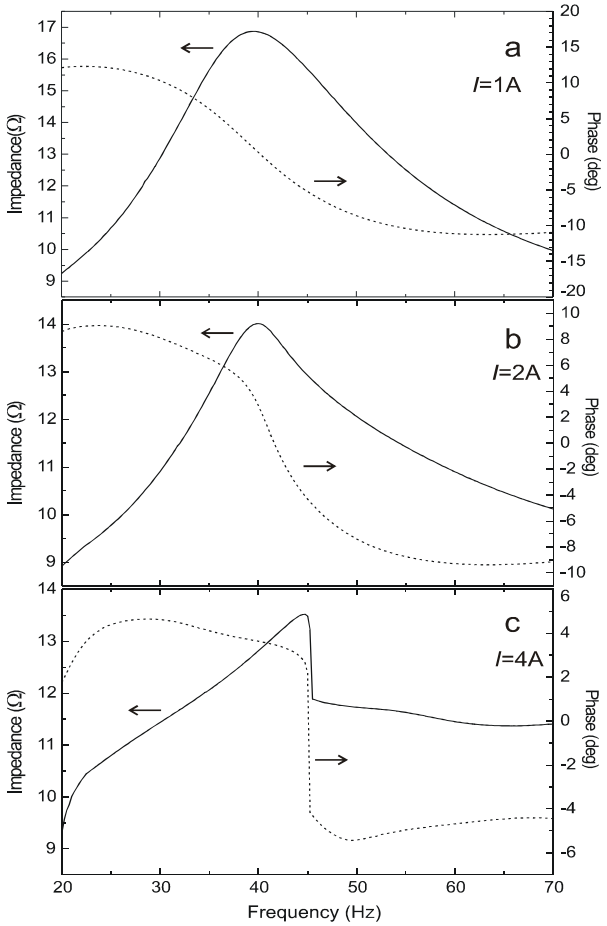

Fig. 6 Impedance curve for various excitation currents

2.1 Experimental chaotic state observation

The experiments included measurements of the loudspeaker displacement amplitudes using laser distance meter. The fixed excitation frequency (f=43 Hz) is just a little lower than frequency where cut-off effect is obtained. Excitation current was increased with rate of 20 mA/sec and displacement amplitude was recorded. From the recorded signal, peak amplitudes were extracted and diagram in figure 7 was obtained.

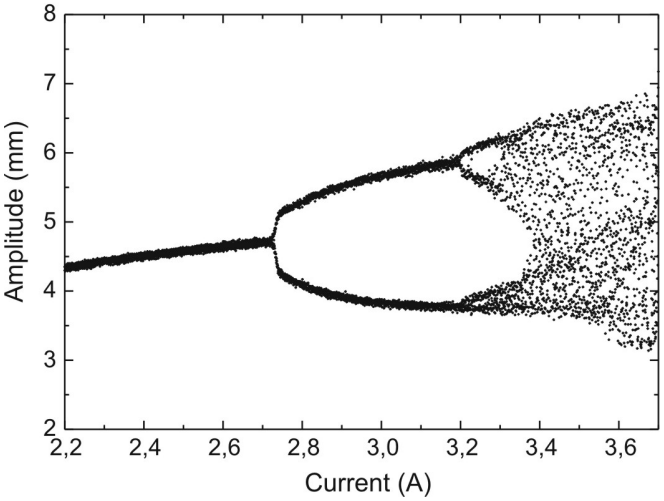

Fig. 7 Peak displacement amplitude vs. excitation current

The vibration amplitude for I_0 = 2.0 A is 6.2 mm and is nearly constant for higher driving currents, while in the current range $0 < I_0 < 100$ mA vibration amplitude increases in the rate 0.052 m/A. It is obvious that amplitude is heavily suppressed at high driving currents, and current dependent friction R_i is insufficient to explain such a suppression, as one might expect.

3 Theoretical chaos modeling

The crucial question is how to model this experimental loudspeaker behaviour.

In some instances, experimental findings appeared in the course of this work call an attention for the contribution of coupled friction-stiffness mechanism.

This connection between stiffness and friction is characteristic property of viscoelastic body incorporated in membrane of EDL unit.

Bennewitz and Rötger [6] (B-R) proposed a rather simple model of the viscoelastic body subjected to the forced oscillation, and the body was supposed to consist of a large number of small viscoelastic regions, each region being the source of the hysteretic local surface deformation. Deformation of the i-th region is relaxed to the equilibrium in time $1/\gamma_i$, and γ_i might be interpreted as viscoelastic resonance frequencies. The equation of membrane motion is superposition of voice coil motion, motions because different modes of loudspeaker membrane (Bessels function) and because of tilts due to viscoelastic membrane properties.

The equation of motion suggested by B-R theory is rather complicated but it can be reduced to the form of eq. 3 when mean statistical value of relaxing time is same $\gamma_i = \gamma$.

$$\frac{d^3y}{dt^3} + \gamma \cdot \frac{d^2y}{dt^2} + \omega_0^2 \cdot \left(1 + \frac{\beta \cdot \delta}{E}\right) \cdot \frac{dy}{dt} + \omega_0^2 \cdot \gamma \cdot y = F \quad (3)$$

It can be seen that viscoelastic parameter γ is responsible for strong effective stiffness nonlinearity.

Assuming strong effective stiffness nonlinearity after displacement amplitude of 5 mm, the EDL nonlinear dynamics behaviour shown in experiments can be explained theoretically solving Duffing equation numerically, using MATLAB Runge-Kutta ODE solver.

3.1 Numerically solving nonlinear 1-D equation

A systematic approach to describing loudspeaker vibrating system, using the Duffing equation, was provided by Woafo [7], where it has been shown that related models of electromechanical transducers may exhibit chaos. However, Woafo also noted that a linear version is used to describe loudspeakers, and that nonlinear terms, which are known to cause subharmonics, are often neglected.
The effective stiffness is assumed in two different forms, <with small and strong nonlinearity (figures 8 and 9).

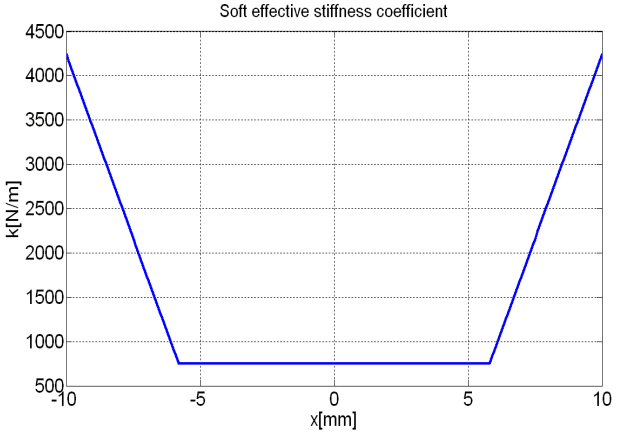

Fig. 8 Soft effective stiffness nonlinearity assumed in theoretical experiments.

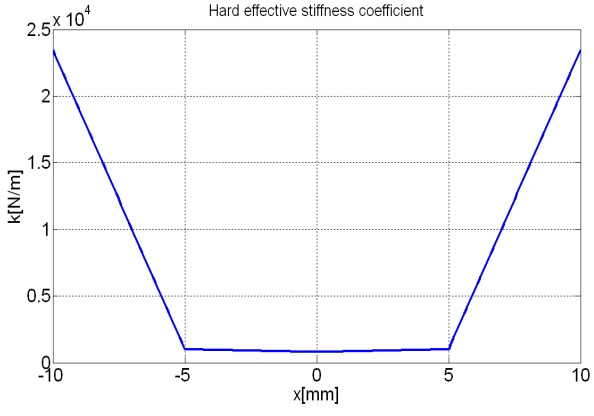

Fig. 9 Hard effective stiffness nonlinearity assumed in theoretical experiments

The nonlinear equation in the Duffing form, with only nonlinear effective stiffness spatial dependency, in the form of Equation 4 has been solved numerically using Runge-Kutta numerical procedure implemented in MATLAB function *ode23*.

$$M_{eff} \cdot \frac{d^2x}{dt^2} + R_m \cdot \frac{dx}{dt} + k_{eff}(x) \cdot x = B \cdot l \cdot I_0 \cdot \cos(\omega \cdot t) \qquad (4)$$

Effective mass of loudspeaker is assumed constant M_{eff}=16 g, same as mechanical losses R_m= 0.41 kg/s and factor $B \cdot l$=5.5 Tm was obtained from manufacturer's data.
The current magnitude is changed in the range of currents used in real world experiments (I_0=2-3 A). The excitation frequency is chosen few Hertz below cut-off frequency observed in theoretical simulations (f= 43 Hz).
The current magnitude is changed with resolution of 0.005 A. The displacement and velocity steady-state waveforms are found for each excitation current magnitude in the time interval from 0 to 0.1 s. The waveforms are sampled with sampling frequency f_S= 2 kHz which is high enough for satisfying Nyquist law, even when twentieth von Karman harmonic of the current excitation frequency ($20 \cdot f$= 860Hz) appears in the displacement signal due to effective stiffness nonlinearity.
The displacement magnitude in steady state for each excitation current magnitude is recorded in the time point when excitation current has maximum value ($cos(\omega \cdot t)$ at maximum). This enables plotting the so called brute-force diagram, displacement magnitude in the moment t, when excitation current has maximum versus current magnitude. The initial conditions for new current magnitude simulations are chosen from the last integration point of previous simulation parameter I_0.
The obtained results are sensitive on initial conditions, duration of simulations for each current magnitude and loudspeaker parameters. The results are shown for soft and hard effective stiffness nonlinearity.
Poincaré map of considered system has been plotted recording displacement and velocity magnitude at excitation current in brute force diagram when chaotic state appear in simulations.

The periodic forcing on the right-hand side of the Duffing equation causes the problem that the system's state (x, dx/dt, t) explicitly contains the variable t, which is non-periodic and unbounded. This makes it difficult to define an event function for a Poincaré section.

A typical solution to this problem is to extend the periodically forced equation by a system that has $\sin(\omega \cdot t)$ and $\cos(\omega \cdot t)$ as its solution and to replace the forcing term with the correct solution components (eq. 5 and 6).

$$\dot{u} = u + \omega \cdot v - u \cdot (u^2 + v^2) \qquad (5)$$

$$\dot{v} = -\omega \cdot u + v - v \cdot (u^2 + v^2) \qquad (6)$$

The sub-system in u and v has the solution $u(t)=\sin(\omega \cdot t)$ and $v(t)=\cos(\omega \cdot t)$. This is now an autonomous system and it's state (x, dx/dt, u, v) has only variables periodic in *time*. It is now easy to specify an event function that becomes zero if excitation current signal has maximum. The simulation results for assumed soft effective stiffness nonlinearity are shown on figure 10.

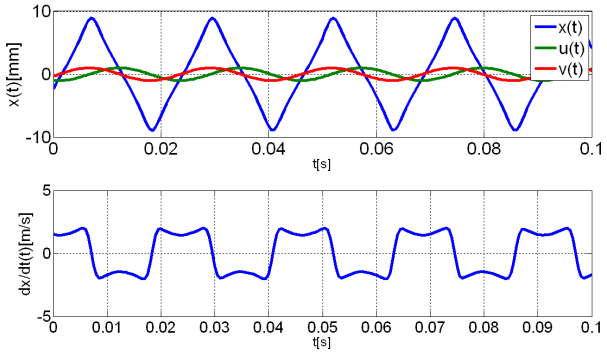

Fig. 10 Displacement and velocity amplitude with soft nonlinearity included in the system

When soft nonlinearity is present in the system only von Karman harmonics can be obtained in displacement for current magnitude used in real world experiments.

The results of theoretical experiments for hard stiffness nonlinearity are shown in the following figures. The brute force diagram is shown on figure 11 in the range of current magnitudes from 2.5 A to 3A.

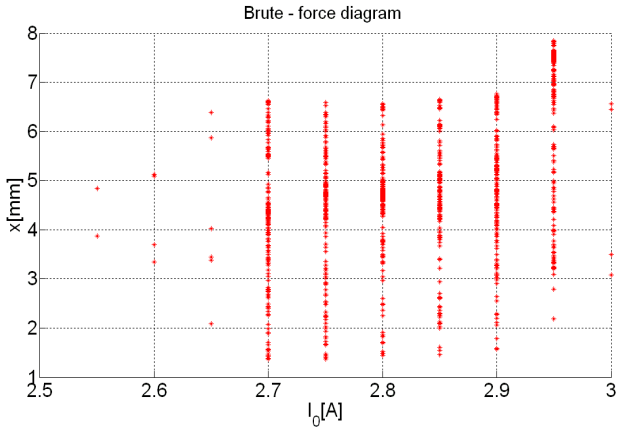

Fig. 11 Brute force diagram for hard nonlinearity effective stiffness simulations

It can be seen that chaotic behaviour appears in theoretically modeled system at current magnitude I_0= 2.7 A.

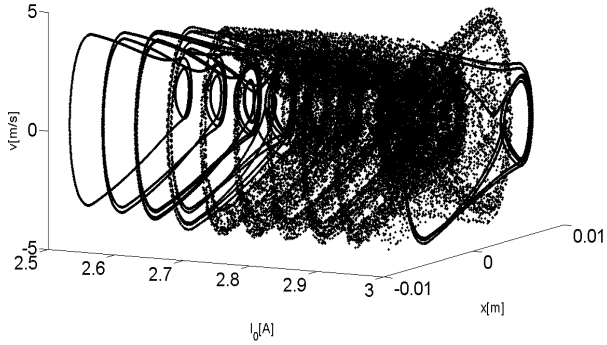

Fig. 12 The velocity and displacement phase plot vs. current magnitude

When model exhibits chaotic behaviour the large number of orbits can be seen on figure 12.
The displacement and velocity waveforms and excitation current help functions $u(t)$ and $v(t)$ are shown on figure 13..
The displacement and velocity magnitude for brute force

diagram and Poincaré map is recorded at time when current function has maximum.

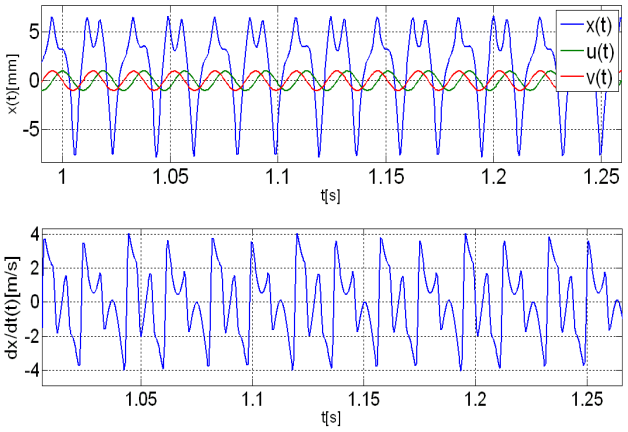

Fig. 13 Displacement and velocity waveforms obtained with numerical simulations in chaotic state.

The Poincare map recorded when current magnitude is 2.7 A and excitation frequency f= 43 Hz is shown on figure 14.

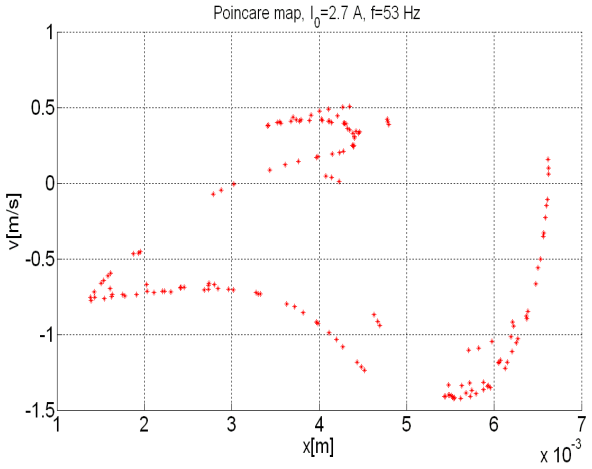

Fig. 14 Poincare map obtained in theoretical simulations

4 Conclusion

An experimental evidence and brief theoretical explanation of the chaotic state in an electrodynamic loudspeaker have been presented. The new model of viscoelastic coupling between membrane stiffness and losses is proposed for theoretically explanation of observed phenomena. Chaotic state cannot be explained with effective stiffness nonlinearity measured with classical methods. The coupling of intrinsic membrane friction to the elastic stiffness has been verified by analysis of Bennewitz-Rötger equation dealing with vibration of a viscoelastic body. The further steps will be analysis of membrane displacement amplitude waveforms with appropriate time series analysis.

References

[1] D. Davis and E. Patronis, *Sound System Engineering*, Third edition: Elsevier, 2006

[2] A. Petošić, I. Djurek and D. Djurek, Modeling of an electrodynamic loudspeaker using Runge-Kutta ODE solver, 122nd AES Convention Vienna, May 5-8, 2007. Convention paper

[3] I. Djurek, A. Petosic and D. Djurek, Mass nonlinearity and intrinsic friction of the loudspeaker membrane, 122nd AES Convention Vienna, May 5-8, 2007. Convention paper 7075

[4] M.H. Knudsen, P. Hansen and J. Grunsen, The significance of viscoelastic effects in loudspeaker parameter measurements, 88th AES Convention, Montreux, March, 13-16, 1990. Convention paper 2905.

[5] A. Petošić, I. Djurek and D. Djurek: Modeling of an electrodynamic loudspeaker including membrane viscoelasticity, AES Convention Amsterdam, May 17-29, 2008. Convention paper 7075

[6] K. Bennewitz and H. Rötger, Ueber die innere Reibung fester Körper;Absorptionsfrequenzen von Metallen im akustischen Gebiet, Physik. Zeitschr. **37** (1936) 578-588.

[7] P. Woafo, Harmonic oscillations, stability and chaos control in a non-linear electromechanical system, Journal of Sound and Vibration, vol. 259, pp. 1253–1264, 2003.